Fractional scale transform and fractional Mellin transform for scale, rotation, and translation invariant pattern recognition to discriminate between 30 phytoplankton species

E. Garza-Flores and J. Álvarez-Borrego

Centro de Investigación Científica y Educación Superior de Ensenada, B. C., División de Física Aplicada, Departamento de óptica, Carretera Ensenada-Tijuana 3918, Fracc. Zona Playitas, 22860, B. C., México.

Received 3 October 2025; accepted 1 May 2026

The fractional scale transform is introduced and studied to develop a new pattern recognition system invariant to scale, translation, and rotation. This system was also implemented with the fractional Mellin transform, and the results were compared with those obtained with the fractional scale transform. The analysis was performed to classify 30 phytoplankton species. For both transformations, optimal orders were found for each species. This study implemented nonlinear correlation and adaptive nonlinear correlation for the classification stage. The system achieved a mean accuracy of 0.998 with nonlinear correlation and 0.999 with adaptive nonlinear correlation.

Keywords: Computer vision; fractional Mellin transform; fractional scale transform; pattern recognition; phytoplankton.

DOI: https://doi.org/10.31349/RevMexFis.72.051301

1. Introduction

The fractional Fourier transform (FrFT), as a generalization of the conventional Fourier Transform (FT), has found applications in different areas where the FT has been used, with the potential to obtain better results [1]. Image correlation using FrFT or fractional correlation has been used for object recognition [2], showing a less noisy response than conventional correlation. Likewise, for identifying 30 phytoplankton species, a pattern recognition methodology invariant to translation and rotation was developed based on one-dimensional signatures obtained with binary masks generated from the FrFT, which were classified using nonlinear correlation [3]. In this methodology, FrFT orders were found for each species, which improved discrimination capacity compared to the case in which the FT is used for mask generation.

In addition to the FrFT, the concept of fractional orders has been extended to other transforms, including the Mellin transform (MT), giving rise to the fractional Mellin transform (FrMT) [4]. Butzer *et al*. (2002) conducted an extensive study of fractional Mellin analysis, using the so-called Hadamard integrals [5-7]. The MT can be implemented via the FT, also known as the Fourier-Mellin transform [8,9]. However, by working with the FrFT, the FrMT can be obtained, also called the fractional Fourier-Mellin transform. Sazbon *et al*. (2002) implemented optical correlators based on the fractional Fourier-Mellin transform for navigation tasks to detect and control specific ranges of object motion [10]. In 2011, Sharma showed how the fractional Fourier-Mellin transform is a generalization of the conventional Fourier-Mellin transform [11]. Zuo and Zhou (2011) performed spectrum analysis with the MT and FrMT, finding that the fractional version preserves the scale-invariance property [12]. Zhou *et al*. (2012) applied the MT to develop a reality-preserving color encryption algorithm [13]. Vashisth *et al*. (2014) implemented a phase mask for encryption, based on the fractional Mellin transform [14]. In 2015, Sharma and Deshmukh proved the analyticity of the FrMT [15]. Baloch *et al*. (2019) established the relationship that the FrMT also has with the fractional Laplace transform [16]. Wang *et al*. (2020) presented an encryption scheme based on the reality-preserving FrMT with Gaussian opening [17].

Furthermore, Cohen proposed the concept of scale transform (ST) in 1993. In this transformation, the main magnitude to be represented is, as its name indicates, the scale, since scale can be considered as a physical attribute of a signal [18]. Like the MT, this transform has the property that its modulus is invariant to changes in scale, in the same way that the modulus of the FT is invariant to translation. Also, like the MT, this transformation can be implemented digitally, through the FT using a logarithmic mapping [19].

To enhance discriminative capabilities in image classification problems regardless of scale, rotation, and translation changes, this work proposes the fractional scale transform (FrST) by extending the concept of fractional orders to the ST. To achieve this, the FrFT is employed. In addition to the FrST, the FrMT was also implemented for classification using nonlinear and adaptive nonlinear correlations.

The rest of the article is organized as follows. In Sec. 2, the mathematical theory behind this work is presented. The methodology is described in Sec. 3. Section 4 presents the analysis and results, and finally, in Sec. 5, the conclusion is given.

2. Mathematical bases

2.1. The MT

The MT is an integral transform strongly related to the FT. The MT of a function is defined as

$$M(s) = \int_0^\infty f(x) x^{s-1} dx, \quad (1)$$

where, $s = jc + \beta$ and c is the scale variable. Equation (1) defines the β-Mellin transform family. If $\beta = 0$ we obtain a compression/expansion invariant transform [20], in this case

$$M(c) = \mathcal{M}\{f(x)\} = \int_0^\infty f(x) x^{-jc-1} dx. \quad (2)$$

The most useful property of the MT with $\beta = 0$ is that any change in scale in the spatial domain translates to a change only in phase in the Mellin domain, while its modulus remains invariant to those changes in scale. For the case of an image, the two-dimensional MT is used, which is given by [21]

$$\mathcal{M}\{f(x,y)\} = \int_0^\infty \int_0^\infty f(x,y) x^{-ju-1} y^{-jv-1} dx dy. \quad (3)$$

2.2. The scale transform

The scale transform (ST) is a special case of the MT with $\beta = 1/2$. The ST is given by [18]

$$D(c) = \mathcal{D}\{f(x)\} = \frac{1}{\sqrt{2\pi}} \int_0^\infty f(x) \frac{e^{-jclnx}}{\sqrt{x}} dx. \quad (4)$$

Equation (4) can also be written as

$$\mathcal{D}\{f(x)\} = \frac{1}{\sqrt{2\pi}} \int_0^\infty f(x) x^{-jc-\frac{1}{2}} dx, \quad (5)$$

which is equivalent to the MT with complex argument $s = -jc + 1/2$. In two dimensions, the scale transform is given by [22]

$$\mathcal{D}\{f(x,y)\} = \frac{1}{\sqrt{2\pi}} \int_0^\infty \int_0^\infty f(x,y) \times \frac{e^{-jc_x lnx - jc_y lny}}{\sqrt{xy}} dx dy. \quad (6)$$

2.3. Relationship between the MT and the ST

The MT in Eq. (2) can also be written as

$$\mathcal{M}\{f(x)\} = \int_0^\infty \frac{f(x) x^{-jc}}{x} dx, \quad (7)$$

while the ST in Eq. (4) can be expressed as

$$\mathcal{D}\{f(x)\} = \frac{1}{\sqrt{2\pi}} \int_0^\infty \frac{f(x) x^{-jc}}{\sqrt{x}} dx. \quad (8)$$

Therefore, discarding the constant $1/\sqrt{2\pi}$, which is only for normalization purposes, there is a relationship between the MT and the ST, given by [23]

$$\mathcal{M}\{\sqrt{x} f(x)\} = \mathcal{D}\{f(x)\}. \quad (9)$$

2.4. FrMT and FrST

The FrMT is a generalization of the MT as the FrFT is to the FT. The two-dimensional FrMT of the order p of the function $f(x,y)$ is defined by [24]

$$\mathcal{M}^p\{f(x,y)\} = \mathcal{M}_\alpha\{f(x,y)\} = \int_0^\infty \int_0^\infty f(x,y) \times K_\alpha(x,y,u,v) dx dy, \quad (10)$$

where the kernel $K_\alpha(x,y,u,v)$ is defined by

$$K_\alpha(x,y,u,v) = x^{\frac{2\pi uj}{\sin\alpha}-1} y^{\frac{2\pi vj}{\sin\alpha}-1} \times e^{\frac{\pi j}{\tan\alpha}[u^2+v^2+\ln x^2+\ln y^2]}, \quad (11)$$

for $0 < \alpha \leq \pi/2$, and the fractional order is $p = \alpha/(\pi/2)$.

The MT can be implemented via the FT [20] using logarithmic mapping. However, as the FrFT is a generalization of the FT, the fractional concept was also extended to the MT [4]. Therefore, the FrMT can be obtained by implementing the FrFT after the logarithmic mapping [10]. And based on the relationship between the MT and the ST given in Eq. (9), the fractional scale transform can be obtained by multiplying the input by the factor $\sqrt{xy}$ as

$$\mathcal{D}^p\{f(x,y)\} = \mathcal{M}^p\{\sqrt{xy} f(x,y)\}. \quad (12)$$

3. Methodology

In this work, two position, rotation and scale methodologies are presented. In the first method, the FrST is used. The fractional version of the scale transform is implemented using the FrFT. Then, the FrMT is also implemented to compare with the results obtained with the FrST.

3.1. Position, rotation and scale invariant correlation methodology based on the FrST

The system implementing the FrST is shown in the diagram of Fig. 1. It is based on the methodology used to obtain the ST [19], but now using the FrFT instead of the FT to implement the FrST. First, step (1) presents a target image to the system. In step (2), the modulus of the FT, named as the spectral image, is calculated, thus introducing translation invariance. After that, the factor $\sqrt{xy}$ that differentiates the FrST from the FrMT is introduced in step (3). Then, in step (4), the Cartesian coordinates are mapped to polar coordinates, thus obtaining rotation invariance [9,25]. In step (5), a logarithmic mapping is performed. In step (6), the FrST of order p of the target image is obtained by applying the FrFT to the logarithmically scaled data. Then, to get scale invariance, the modulus of the FrST of the target image is calculated in step (7). In step (8), a problem image $g(x,y)$ is introduced to the system, and from step (9) to step (14), the modulus of the FrST of the problem image is calculated. Finally, in step (15), the correlation of the modulus of the FrFTs of the target and problem images is performed to classify the images.

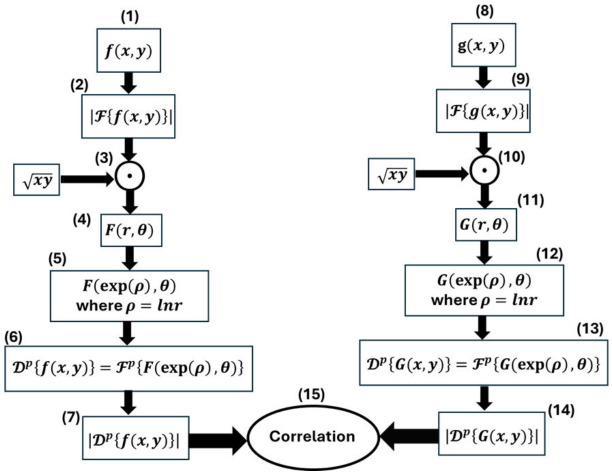

FIGURE 1. Block diagram of the position, rotation, and scale correlation methodology based on the FrST.

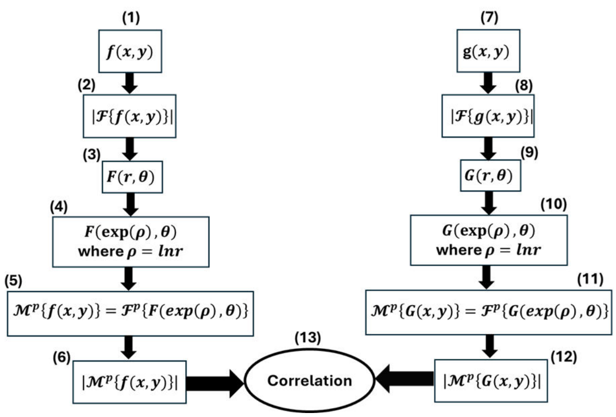

FIGURE 2. Block diagram of the position, rotation, and scale correlation methodology based on the FrMT.

3.2. Position, rotation and scale invariant correlation methodology based on the FrMT

Now, Fig. 2 shows the system implementing the FrMT. In step (1), a target image $f(x,y)$ is presented. In step (2), the spectral image is calculated. Then, in step (3), the Cartesian coordinates are mapped to polar coordinates. In step(4), a logarithmic mapping is performed. In step (5), the FrMT of the order p of the target image is obtained, and its modulus is calculated in step (6). Then, in step (7), a problem image is introduced. From step (8) to step (12), the modulus of the FrMT of the problem image is obtained. Finally, in step (13), the correlation of the modulus of the FrMTs of the target and problem images is calculated.

3.3. Correlation

In the classification stage, using the FrST or the FrMT, nonlinear and adaptative nonlinear correlations are used. The nonlinear correlation or k-law correlation is defined as [26]

$$C_{NL}=\mathcal{F}^{-1}\{|\mathcal{F}\{P_{FR}\}|^k e^{i\phi_{P_{FR}}}|\mathcal{F}\{T_{FR}\}|^k e^{-i\phi_{T_{FR}}}\}, \quad (13)$$

where, for this work $\phi_{P_{FR}}$ and $\phi_{T_{FR}}$ are the phases of the FT of the fractional transformations of the problem image and target image, respectively, and $0 < k < 1$ is the nonlinearity factor. For this work, $k = 0.3$. The adaptative nonlinear correlation is a variation of the nonlinear correlation that gives better classification performance, and is defined as [27]

$$C_{NL} = \mathcal{F}^{-1}\{|\mathcal{F}\{P_{FR}\}|^{k\bullet R} \times e^{i\phi_{P_{FR}}}|\mathcal{F}\{T_{FR}\}|^k e^{-i\phi_{T_{FR}}}\}, \quad (14)$$

where R is the factor that modifies the nonlinearity of the modulus of the FT of the fractional transformation of the problem image. For this work, the R factor is defined as

$$R = \begin{cases} \frac{\sigma(x,y)_{PI}}{\sigma(x,y)_{TI}}, \sigma(x,y)_{PI} \le \sigma(x,y)_{TI}, \\ \frac{\sigma(x,y)_{TI}}{\sigma(x,y)_{PI}}, \sigma(x,y)_{PI} > \sigma(x,y)_{TI}, \end{cases} \quad (15)$$

where $\sigma(x,y)_{PI}$ is the standard deviation of the spectral image of the problem image, and $\sigma(x,y)_{TI}$ is the standard deviation of the spectral image of the target image. Calculating an autocorrelation makes $R = 1$, which turns the adaptative nonlinear correlation into a nonlinear correlation.

4. Analysis and results

This work discriminates between the 30 phytoplankton species in Fig. 3. The classification is made by implementing the FrST or the FrMT with an optimal order.

4.1. Obtaining the optimal order

As stated earlier, the parameter α can have values between 0 and $\pi/2$. Thus, the order p can have values between 0 and 1.

Therefore, it is necessary to determine the optimal value of p to use in the process.

A non-normalized autocorrelation is performed for a particular order p, and the peak value is extracted. This is done for different orders. In this way, each order will give its respective autocorrelation value. Finally, the order with the highest correlation value is considered the optimal order [3]. This is done for the FrST and the FrMT for all 30 species. The optimal order is searched by changing p from 0.01 to 1 with steps of 0.01. In this way, planes other than the ST and MT are selected, which are special cases of their fractional versions when $p = 1$. Table I shows the optimal order of each species obtained for the FrST and the FrMT. It can be observed that there is no single optimal order for all species, and in some cases, the optimal order of a species differs for each transformation. Also, for both transforms, no species has an optimal order equal to 1. This means that the species identified themselves better in both cases when working with fractional orders.

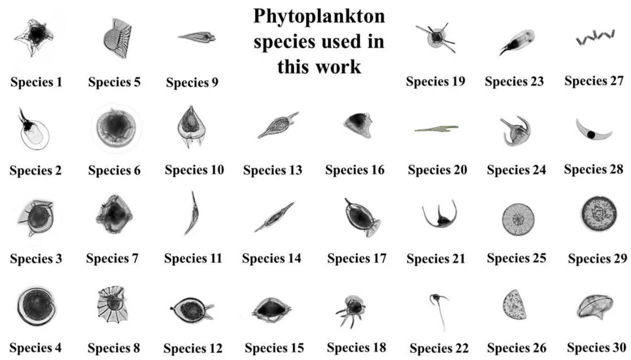

FIGURE 3. Images of the 30 phytoplankton species used in this work. Species 1: *Acanthogonyaulax spinifera*. Species 2: *Ceratium gravidum Gourret*. Species 3: *Dinophysis hastata*. Species 4: *Diplosalopsis orbicularis*. Species 5: *Histioneis*. Species 6: *Lingulodinium polyedrum*. Species 7: *Ornithocercu armata*. Species 8: *Ornithocercus magnificus*. Species 9: *Oxytoxum scolopax*. Species 10: *Podolampas bipes*. Species 11: *Podolampas spinifer*. Species 12: *Podolampas bipes*. Species 13: *Podolampas palmipes*. Species 14: *Podolampa spinifer*. Species 15: *Protoperidinium. Species* 16: *Dinophysis rapa*. Species 17: *Dinophysis hastate*. Species 18: *Ceratocorys horrida*. Species 19: *Ceratocorys horrida*. Species 20: *Ceratium furca*. Species 21: *Ceratium lunula*. Species 22: *Ceratium hexacanthum*. Species 23: *Ceratium praelongum*. Species 24: *Ceratium breve*. Species 25: *Asterolampra marylandica*. Species 26: *Hemidiscus cuneiformis*. Species 27: *Thalassionema nitzschioides*. Species 28: *Pyrocystis*. Species 29: *Hemidiscus*. Species 30: *Dinoflagellata*.

4.2. Classification

Thirty species of phytoplankton were used to analyze the performance of the two correlation methodologies invariant to position, rotation and scale presented in this work. The images are grayscale with a 307×307 size. Each of the 30 species was scaled $\pm 10\%$ in steps of 1%. Thus, the scale ranges from 90% to 110% of the original image (100% scale); this range is typical of this species type, which is why the range was selected. Therefore, considering the original image, 21 scaled versions were produced for each species. Then, the original image of each species was selected as the target and compared with all scaled versions of itself and all scaled versions of the other species. The comparison was made by following the transformation methodologies described in Secs. 3.1 and 3.2. The order used in each comparison was that of the target species, depending on the transformation used, as shown in Table I. This process was performed using non-linear correlation and adaptative non-linear correlation for both transformations. Figures 4 and 5 show the results obtained with the FrST and the FrMT when species 4 is the target. The box plots show the mean. ± 1 standard deviation, and the maximum and minimum values obtained from all the performed correlations.

Figure 4a) shows the results of the nonlinear correlation with the FrST. Considering the maximum and minimum values in the box plots, there is some overlap with species 25 only. Figure 4b) shows the results for the same transformation but using adaptive nonlinear correlation, with no overlaps. The results for the FrMT transform using nonlinear correlation are shown in Fig. 5a), and those with adaptive nonlinear correlation are shown in Fig. 5b), with no overlap in either case. To evaluate the performance with each species as the target, four metrics were used:

$$\text{accuracy}(S_n) = \frac{TP_n + TN_n}{TP_n + TN_n + FP_n + FN_n}, \qquad (16)$$

$$\text{sensitivity}(S_n) = \frac{TP_n}{TP_n + FN_n}, \qquad (17)$$

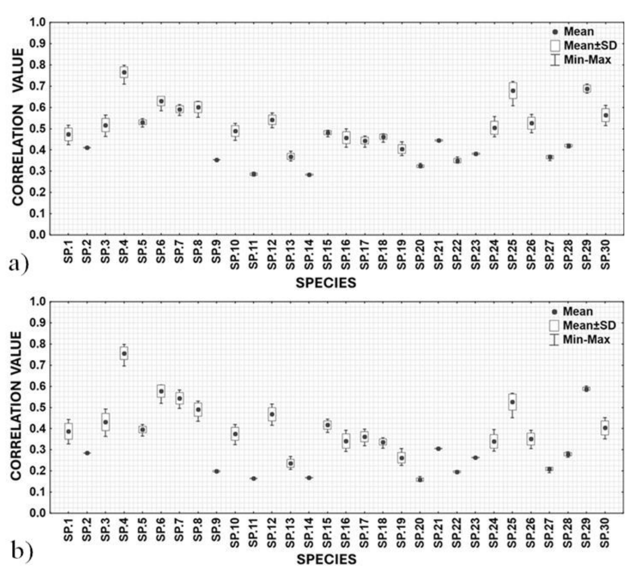

FIGURE 4. Results obtained by implementing the FrST using species four as the target. a) Nonlinear correlation. b) Adaptative nonlinear correlation.

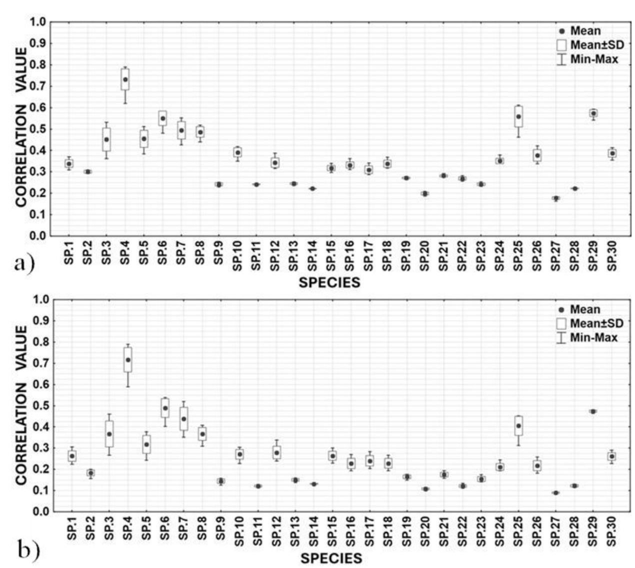

FIGURE 5. Results obtained by implementing the FrMT using species four as the target. a) Nonlinear correlation. b) Adaptative nonlinear correlation.

TABLE I. Optimal order for each phytoplankton species. Column 1 shows results obtained with FrST. Column 2 shows results obtained with FrMT.

Species	FrST optimal orders	FrMT optimal orders
1	0.986	0.986
2	0.991	0.991
3	0.978	0.978
4	0.978	0.953
5	0.979	0.986
6	0.978	0.978
7	0.978	0.952
8	0.979	0.979
9	0.986	0.986
10	0.986	0.986
11	0.993	0.992
12	0.978	0.978
13	0.984	0.984
14	0.974	0.974
15	0.985	0.985
16	0.985	0.978
17	0.978	0.978
18	0.986	0.986
19	0.986	0.986
20	0.977	0.978
21	0.978	0.978
22	0.985	0.985
23	0.983	0.984
24	0.978	0.978
25	0.978	0.978
26	0.985	0.979
27	0.978	0.978
28	0.978	0.978
29	0.978	0.978
30	0.979	0.978

TABLE II. Results of the FrST with nonlinear correlation.

Species	Accuracy	Sensitivity	Specificity	Precision
1	1	1	1	1
2	1	1	1	1
3	1	1	1	1
4	0.995	0.905	0.998	0.950
5	1	1	1	1
6	0.995	0.857	1	1
7	1	1	1	1
8	1	1	1	1
9	1	1	1	1
10	1	1	1	1
11	1	1	1	1
12	1	1	1	1
13	1	1	1	1
14	1	1	1	1
15	1	1	1	1
16	1	1	1	1
17	1	1	1	1
18	1	1	1	1
19	1	1	1	1
20	1	1	1	1
21	1	1	1	1
22	1	1	1	1
23	1	1	1	1
24	1	1	1	1
25	0.976	0.571	0.990	0.667
26	1	1	1	1
27	1	1	1	1
28	1	1	1	1
29	0.982	0.905	0.985	0.679
30	1	1	1	1
AVERAGE	**0.998**	**0.974**	**0.999**	**0.976**

Confusion Matrix

True Label

Species	1	2	3	4	5	6	7	8	9	10	11	12	13	14	15	16	17	18	19	20	21	22	23	24	25	26	27	28	29	30
1	21	0	0	0	0	0	0	0	0	0	0	0	0	0	0	0	0	0	0	0	0	0	0	0	0	0	0	0	0	0
2	0	21	0	0	0	0	0	0	0	0	0	0	0	0	0	0	0	0	0	0	0	0	0	0	0	0	0	0	0	0
3	0	0	21	0	0	0	0	0	0	0	0	0	0	0	0	0	0	0	0	0	0	0	0	0	0	0	0	0	0	0
4	0	0	0	19	0	0	0	0	0	0	0	0	0	0	0	0	0	0	0	0	0	0	0	0	2	0	0	0	0	0
5	0	0	0	0	21	0	0	0	0	0	0	0	0	0	0	0	0	0	0	0	0	0	0	0	0	0	0	0	0	0
6	0	0	0	1	0	18	0	0	0	0	0	0	0	0	0	0	0	0	0	0	0	0	0	0	2	0	0	0	0	0
7	0	0	0	0	0	0	21	0	0	0	0	0	0	0	0	0	0	0	0	0	0	0	0	0	0	0	0	0	0	0
8	0	0	0	0	0	0	0	21	0	0	0	0	0	0	0	0	0	0	0	0	0	0	0	0	0	0	0	0	0	0
9	0	0	0	0	0	0	0	0	21	0	0	0	0	0	0	0	0	0	0	0	0	0	0	0	0	0	0	0	0	0
10	0	0	0	0	0	0	0	0	0	21	0	0	0	0	0	0	0	0	0	0	0	0	0	0	0	0	0	0	0	0
11	0	0	0	0	0	0	0	0	0	0	21	0	0	0	0	0	0	0	0	0	0	0	0	0	0	0	0	0	0	0
12	0	0	0	0	0	0	0	0	0	0	0	21	0	0	0	0	0	0	0	0	0	0	0	0	0	0	0	0	0	0
13	0	0	0	0	0	0	0	0	0	0	0	0	21	0	0	0	0	0	0	0	0	0	0	0	0	0	0	0	0	0
14	0	0	0	0	0	0	0	0	0	0	0	0	0	21	0	0	0	0	0	0	0	0	0	0	0	0	0	0	0	0
15	0	0	0	0	0	0	0	0	0	0	0	0	0	0	21	0	0	0	0	0	0	0	0	0	0	0	0	0	0	0
16	0	0	0	0	0	0	0	0	0	0	0	0	0	0	0	21	0	0	0	0	0	0	0	0	0	0	0	0	0	0
17	0	0	0	0	0	0	0	0	0	0	0	0	0	0	0	0	21	0	0	0	0	0	0	0	0	0	0	0	0	0
18	0	0	0	0	0	0	0	0	0	0	0	0	0	0	0	0	0	21	0	0	0	0	0	0	0	0	0	0	0	0
19	0	0	0	0	0	0	0	0	0	0	0	0	0	0	0	0	0	0	21	0	0	0	0	0	0	0	0	0	0	0
20	0	0	0	0	0	0	0	0	0	0	0	0	0	0	0	0	0	0	0	21	0	0	0	0	0	0	0	0	0	0
21	0	0	0	0	0	0	0	0	0	0	0	0	0	0	0	0	0	0	0	0	21	0	0	0	0	0	0	0	0	0
22	0	0	0	0	0	0	0	0	0	0	0	0	0	0	0	0	0	0	0	0	0	21	0	0	0	0	0	0	0	0
23	0	0	0	0	0	0	0	0	0	0	0	0	0	0	0	0	0	0	0	0	0	0	21	0	0	0	0	0	0	0
24	0	0	0	0	0	0	0	0	0	0	0	0	0	0	0	0	0	0	0	0	0	0	0	21	0	0	0	0	0	0
25	0	0	0	0	0	0	0	0	0	0	0	0	0	0	0	0	0	0	0	0	0	0	0	0	12	0	0	0	9	0
26	0	0	0	0	0	0	0	0	0	0	0	0	0	0	0	0	0	0	0	0	0	0	0	0	0	21	0	0	0	0
27	0	0	0	0	0	0	0	0	0	0	0	0	0	0	0	0	0	0	0	0	0	0	0	0	0	0	21	0	0	0
28	0	0	0	0	0	0	0	0	0	0	0	0	0	0	0	0	0	0	0	0	0	0	0	0	0	0	0	21	0	0
29	0	0	0	0	0	0	0	0	0	0	0	0	0	0	0	0	0	0	0	0	0	0	0	0	2	0	0	0	19	0
30	0	0	0	0	0	0	0	0	0	0	0	0	0	0	0	0	0	0	0	0	0	0	0	0	0	0	0	0	0	21

Predicted Label

FIGURE 6. Confusion matrix obtained with the FrST using nonlinear correlation. Rows represent true classes, while columns represent the predicted classes.

Confusion Matrix

True Label / Predicted Label

Species	1	2	3	4	5	6	7	8	9	10	11	12	13	14	15	16	17	18	19	20	21	22	23	24	25	26	27	28	29	30
1	21	0	0	0	0	0	0	0	0	0	0	0	0	0	0	0	0	0	0	0	0	0	0	0	0	0	0	0	0	0
2	0	21	0	0	0	0	0	0	0	0	0	0	0	0	0	0	0	0	0	0	0	0	0	0	0	0	0	0	0	0
3	0	0	21	0	0	0	0	0	0	0	0	0	0	0	0	0	0	0	0	0	0	0	0	0	0	0	0	0	0	0
4	0	0	0	21	0	0	0	0	0	0	0	0	0	0	0	0	0	0	0	0	0	0	0	0	0	0	0	0	0	0
5	0	0	0	0	21	0	0	0	0	0	0	0	0	0	0	0	0	0	0	0	0	0	0	0	0	0	0	0	0	0
6	0	0	0	0	0	21	0	0	0	0	0	0	0	0	0	0	0	0	0	0	0	0	0	0	0	0	0	0	0	0
7	0	0	0	0	0	0	21	0	0	0	0	0	0	0	0	0	0	0	0	0	0	0	0	0	0	0	0	0	0	0
8	0	0	0	0	0	0	0	21	0	0	0	0	0	0	0	0	0	0	0	0	0	0	0	0	0	0	0	0	0	0
9	0	0	0	0	0	0	0	0	21	0	0	0	0	0	0	0	0	0	0	0	0	0	0	0	0	0	0	0	0	0
10	0	0	0	0	0	0	0	0	0	21	0	0	0	0	0	0	0	0	0	0	0	0	0	0	0	0	0	0	0	0
11	0	0	0	0	0	0	0	0	0	0	21	0	0	0	0	0	0	0	0	0	0	0	0	0	0	0	0	0	0	0
12	0	0	0	0	0	0	0	0	0	0	0	21	0	0	0	0	0	0	0	0	0	0	0	0	0	0	0	0	0	0
13	0	0	0	0	0	0	0	0	0	0	0	0	21	0	0	0	0	0	0	0	0	0	0	0	0	0	0	0	0	0
14	0	0	0	0	0	0	0	0	0	0	0	0	0	21	0	0	0	0	0	0	0	0	0	0	0	0	0	0	0	0
15	0	0	0	0	0	0	0	0	0	0	0	0	0	0	21	0	0	0	0	0	0	0	0	0	0	0	0	0	0	0
16	0	0	0	0	0	0	0	0	0	0	0	0	0	0	0	21	0	0	0	0	0	0	0	0	0	0	0	0	0	0
17	0	0	0	0	0	0	0	0	0	0	0	0	0	0	0	0	21	0	0	0	0	0	0	0	0	0	0	0	0	0
18	0	0	0	0	0	0	0	0	0	0	0	0	0	0	0	0	0	21	0	0	0	0	0	0	0	0	0	0	0	0
19	0	0	0	0	0	0	0	0	0	0	0	0	0	0	0	0	0	0	21	0	0	0	0	0	0	0	0	0	0	0
20	0	0	0	0	0	0	0	0	0	0	0	0	0	0	0	0	0	0	0	21	0	0	0	0	0	0	0	0	0	0
21	0	0	0	0	0	0	0	0	0	0	0	0	0	0	0	0	0	0	0	0	21	0	0	0	0	0	0	0	0	0
22	0	0	0	0	0	0	0	0	0	0	0	0	0	0	0	0	0	0	0	0	0	21	0	0	0	0	0	0	0	0
23	0	0	0	0	0	0	0	0	0	0	0	0	0	0	0	0	0	0	0	0	0	0	21	0	0	0	0	0	0	0
24	0	0	0	0	0	0	0	0	0	0	0	0	0	0	0	0	0	0	0	0	0	0	0	21	0	0	0	0	0	0
25	0	0	0	0	0	0	0	0	0	0	0	0	0	0	0	0	0	0	0	0	0	0	0	0	20	0	0	0	1	0
26	0	0	0	0	0	0	0	0	0	0	0	0	0	0	0	0	0	0	0	0	0	0	0	0	0	21	0	0	0	0
27	0	0	0	0	0	0	0	0	0	0	0	0	0	0	0	0	0	0	0	0	0	0	0	0	0	0	21	0	0	0
28	0	0	0	0	0	0	0	0	0	0	0	0	0	0	0	0	0	0	0	0	0	0	0	0	0	0	0	21	0	0
29	0	0	0	0	0	0	0	0	0	0	0	0	0	0	0	0	0	0	0	0	0	0	0	0	0	0	0	0	21	0
30	0	0	0	0	0	0	0	0	0	0	0	0	0	0	0	0	0	0	0	0	0	0	0	0	0	0	0	0	0	21

FIGURE 7. Confusion matrix obtained with the FrST using adaptive nonlinear correlation. Rows represent true classes, while columns represent the predicted classes.

TABLE III. Results of the FrST with adaptive nonlinear correlation.

Species	Accuracy	Sensitivity	Specificity	Precision
1	1	1	1	1
2	1	1	1	1
3	1	1	1	1
4	1	1	1	1
5	1	1	1	1
6	1	1	1	1
7	1	1	1	1
8	1	1	1	1
9	1	1	1	1
10	1	1	1	1
11	1	1	1	1
12	1	1	1	1
13	1	1	1	1
14	1	1	1	1
15	1	1	1	1
16	1	1	1	1
17	1	1	1	1
18	1	1	1	1
19	1	1	1	1
20	1	1	1	1
21	1	1	1	1
22	1	1	1	1
23	1	1	1	1
24	1	1	1	1
25	0.998	0.952	1	1
26	1	1	1	1
27	1	1	1	1
28	1	1	1	1
29	0.998	1	0.998	0.955
30	1	1	1	1
AVERAGE	**0.999**	**0.998**	**0.999**	**0.998**

TABLE IV. Results of the FrMT with nonlinear correlation.

Species	Accuracy	Sensitivity	Specificity	Precision
1	1	1	1	1
2	1	1	1	1
3	1	1	1	1
4	0.998	1	0.998	0.955
5	1	1	1	1
6	0.997	0.905	1	1
7	1	1	1	1
8	1	1	1	1
9	1	1	1	1
10	1	1	1	1
11	1	1	1	1
12	1	1	1	1
13	1	1	1	1
14	1	1	1	1
15	1	1	1	1
16	1	1	1	1
17	1	1	1	1
18	1	1	1	1
19	1	1	1	1
20	1	1	1	1
21	1	1	1	1
22	1	1	1	1
23	1	1	1	1
24	1	1	1	1
25	0.979	0.571	0.993	0.750
26	1	1	1	1
27	1	1	1	1
28	1	1	1	1
29	0.980	0.857	0.985	0.667
30	1	1	1	1
AVERAGE	**0.998**	**0.977**	**0.999**	**0.979**

TABLE V. Results of the FrMT with adaptive nonlinear correlation.

Species	Accuracy	Sensitivity	Specificity	Precision
1	1	1	1	1
2	1	1	1	1
3	1	1	1	1
4	1	1	1	1
5	1	1	1	1
6	1	1	1	1
7	1	1	1	1
8	1	1	1	1
9	1	1	1	1
10	1	1	1	1
11	1	1	1	1
12	1	1	1	1
13	1	1	1	1
14	1	1	1	1
15	1	1	1	1
16	1	1	1	1
17	1	1	1	1
18	1	1	1	1
19	1	1	1	1
20	1	1	1	1
21	1	1	1	1
22	1	1	1	1
23	1	1	1	1
24	1	1	1	1
25	0.998	0.952	1	1
26	1	1	1	1
27	1	1	1	1
28	1	1	1	1
29	0.998	1	0.998	0.955
30	1	1	1	1
AVERAGE	**0.999**	**0.998**	**0.999**	**0.998**

$$\text{specificity}(S_n) = \frac{TN_n}{TN_n + FP_n}, \tag{18}$$

$$\text{precision}(S_n) = \frac{TP_n}{TP_n + FP_n}, \tag{19}$$

where TP_n are true positives for the n species, TN_n, are true negatives for the n species, FP_n are false positives for n species, and FN_n are the false negatives for n species.

Tables II and III show the results obtained for the FrST with nonlinear and adaptative nonlinear correlations, respectively. The tables show the accuracy, sensitivity, specificity, and precision obtained with each species. The last row shows the averages of the four metrics. The results show a value of one for the four metrics in almost every species, with nonlinear correlation. In the case of adaptive nonlinear correlation, only two species do not achieve a value of one for the four metrics. Looking at the averages, adaptive nonlinear correlation has slightly better performance in accuracy, sensitivity, and precision than nonlinear correlation, with the same performance in specificity for both types of correlation.

Tables IV and V show the FrMT results with nonlinear and adaptive nonlinear correlation, respectively. For this transformation, working with nonlinear correlation, the results also show a value of one for the four metrics in almost every species. With adaptive nonlinear correlation, only two species do not achieve a value of one for the four metrics. Again, looking at the averages, only in specificity did both types of correlation have the same performance, with a slightly better performance for adaptive nonlinear correlation in the other three metrics.

Comparing both transformations, in the case of nonlinear correlation, both transforms have the same mean accuracy and mean specificity, and for the mean sensitivity and mean

Confusion Matrix

True Label / Predicted Label

Species	1	2	3	4	5	6	7	8	9	10	11	12	13	14	15	16	17	18	19	20	21	22	23	24	25	26	27	28	29	30
1	21	0	0	0	0	0	0	0	0	0	0	0	0	0	0	0	0	0	0	0	0	0	0	0	0	0	0	0	0	0
2	0	21	0	0	0	0	0	0	0	0	0	0	0	0	0	0	0	0	0	0	0	0	0	0	0	0	0	0	0	0
3	0	0	21	0	0	0	0	0	0	0	0	0	0	0	0	0	0	0	0	0	0	0	0	0	0	0	0	0	0	0
4	0	0	0	21	0	0	0	0	0	0	0	0	0	0	0	0	0	0	0	0	0	0	0	0	0	0	0	0	0	0
5	0	0	0	0	21	0	0	0	0	0	0	0	0	0	0	0	0	0	0	0	0	0	0	0	0	0	0	0	0	0
6	0	0	0	1	0	19	0	0	0	0	0	0	0	0	0	0	0	0	0	0	0	0	0	0	1	0	0	0	0	0
7	0	0	0	0	0	0	21	0	0	0	0	0	0	0	0	0	0	0	0	0	0	0	0	0	0	0	0	0	0	0
8	0	0	0	0	0	0	0	21	0	0	0	0	0	0	0	0	0	0	0	0	0	0	0	0	0	0	0	0	0	0
9	0	0	0	0	0	0	0	0	21	0	0	0	0	0	0	0	0	0	0	0	0	0	0	0	0	0	0	0	0	0
10	0	0	0	0	0	0	0	0	0	21	0	0	0	0	0	0	0	0	0	0	0	0	0	0	0	0	0	0	0	0
11	0	0	0	0	0	0	0	0	0	0	21	0	0	0	0	0	0	0	0	0	0	0	0	0	0	0	0	0	0	0
12	0	0	0	0	0	0	0	0	0	0	0	21	0	0	0	0	0	0	0	0	0	0	0	0	0	0	0	0	0	0
13	0	0	0	0	0	0	0	0	0	0	0	0	21	0	0	0	0	0	0	0	0	0	0	0	0	0	0	0	0	0
14	0	0	0	0	0	0	0	0	0	0	0	0	0	21	0	0	0	0	0	0	0	0	0	0	0	0	0	0	0	0
15	0	0	0	0	0	0	0	0	0	0	0	0	0	0	21	0	0	0	0	0	0	0	0	0	0	0	0	0	0	0
16	0	0	0	0	0	0	0	0	0	0	0	0	0	0	0	21	0	0	0	0	0	0	0	0	0	0	0	0	0	0
17	0	0	0	0	0	0	0	0	0	0	0	0	0	0	0	0	21	0	0	0	0	0	0	0	0	0	0	0	0	0
18	0	0	0	0	0	0	0	0	0	0	0	0	0	0	0	0	0	21	0	0	0	0	0	0	0	0	0	0	0	0
19	0	0	0	0	0	0	0	0	0	0	0	0	0	0	0	0	0	0	21	0	0	0	0	0	0	0	0	0	0	0
20	0	0	0	0	0	0	0	0	0	0	0	0	0	0	0	0	0	0	0	21	0	0	0	0	0	0	0	0	0	0
21	0	0	0	0	0	0	0	0	0	0	0	0	0	0	0	0	0	0	0	0	21	0	0	0	0	0	0	0	0	0
22	0	0	0	0	0	0	0	0	0	0	0	0	0	0	0	0	0	0	0	0	0	21	0	0	0	0	0	0	0	0
23	0	0	0	0	0	0	0	0	0	0	0	0	0	0	0	0	0	0	0	0	0	0	21	0	0	0	0	0	0	0
24	0	0	0	0	0	0	0	0	0	0	0	0	0	0	0	0	0	0	0	0	0	0	0	21	0	0	0	0	0	0
25	0	0	0	0	0	0	0	0	0	0	0	0	0	0	0	0	0	0	0	0	0	0	0	0	12	0	0	0	9	0
26	0	0	0	0	0	0	0	0	0	0	0	0	0	0	0	0	0	0	0	0	0	0	0	0	0	21	0	0	0	0
27	0	0	0	0	0	0	0	0	0	0	0	0	0	0	0	0	0	0	0	0	0	0	0	0	0	0	21	0	0	0
28	0	0	0	0	0	0	0	0	0	0	0	0	0	0	0	0	0	0	0	0	0	0	0	0	0	0	0	21	0	0
29	0	0	0	0	0	0	0	0	0	0	0	0	0	0	0	0	0	0	0	0	0	0	0	0	3	0	0	0	18	0
30	0	0	0	0	0	0	0	0	0	0	0	0	0	0	0	0	0	0	0	0	0	0	0	0	0	0	0	0	0	21

FIGURE 8. Confusion matrix obtained with the FrMT using nonlinear correlation. Rows represent true classes, while columns represent the predicted classes.

Confusion Matrix

True Label / Predicted Label

Species	1	2	3	4	5	6	7	8	9	10	11	12	13	14	15	16	17	18	19	20	21	22	23	24	25	26	27	28	29	30
1	21	0	0	0	0	0	0	0	0	0	0	0	0	0	0	0	0	0	0	0	0	0	0	0	0	0	0	0	0	0
2	0	21	0	0	0	0	0	0	0	0	0	0	0	0	0	0	0	0	0	0	0	0	0	0	0	0	0	0	0	0
3	0	0	21	0	0	0	0	0	0	0	0	0	0	0	0	0	0	0	0	0	0	0	0	0	0	0	0	0	0	0
4	0	0	0	21	0	0	0	0	0	0	0	0	0	0	0	0	0	0	0	0	0	0	0	0	0	0	0	0	0	0
5	0	0	0	0	21	0	0	0	0	0	0	0	0	0	0	0	0	0	0	0	0	0	0	0	0	0	0	0	0	0
6	0	0	0	0	0	21	0	0	0	0	0	0	0	0	0	0	0	0	0	0	0	0	0	0	0	0	0	0	0	0
7	0	0	0	0	0	0	21	0	0	0	0	0	0	0	0	0	0	0	0	0	0	0	0	0	0	0	0	0	0	0
8	0	0	0	0	0	0	0	21	0	0	0	0	0	0	0	0	0	0	0	0	0	0	0	0	0	0	0	0	0	0
9	0	0	0	0	0	0	0	0	21	0	0	0	0	0	0	0	0	0	0	0	0	0	0	0	0	0	0	0	0	0
10	0	0	0	0	0	0	0	0	0	21	0	0	0	0	0	0	0	0	0	0	0	0	0	0	0	0	0	0	0	0
11	0	0	0	0	0	0	0	0	0	0	21	0	0	0	0	0	0	0	0	0	0	0	0	0	0	0	0	0	0	0
12	0	0	0	0	0	0	0	0	0	0	0	21	0	0	0	0	0	0	0	0	0	0	0	0	0	0	0	0	0	0
13	0	0	0	0	0	0	0	0	0	0	0	0	21	0	0	0	0	0	0	0	0	0	0	0	0	0	0	0	0	0
14	0	0	0	0	0	0	0	0	0	0	0	0	0	21	0	0	0	0	0	0	0	0	0	0	0	0	0	0	0	0
15	0	0	0	0	0	0	0	0	0	0	0	0	0	0	21	0	0	0	0	0	0	0	0	0	0	0	0	0	0	0
16	0	0	0	0	0	0	0	0	0	0	0	0	0	0	0	21	0	0	0	0	0	0	0	0	0	0	0	0	0	0
17	0	0	0	0	0	0	0	0	0	0	0	0	0	0	0	0	21	0	0	0	0	0	0	0	0	0	0	0	0	0
18	0	0	0	0	0	0	0	0	0	0	0	0	0	0	0	0	0	21	0	0	0	0	0	0	0	0	0	0	0	0
19	0	0	0	0	0	0	0	0	0	0	0	0	0	0	0	0	0	0	21	0	0	0	0	0	0	0	0	0	0	0
20	0	0	0	0	0	0	0	0	0	0	0	0	0	0	0	0	0	0	0	21	0	0	0	0	0	0	0	0	0	0
21	0	0	0	0	0	0	0	0	0	0	0	0	0	0	0	0	0	0	0	0	21	0	0	0	0	0	0	0	0	0
22	0	0	0	0	0	0	0	0	0	0	0	0	0	0	0	0	0	0	0	0	0	21	0	0	0	0	0	0	0	0
23	0	0	0	0	0	0	0	0	0	0	0	0	0	0	0	0	0	0	0	0	0	0	21	0	0	0	0	0	0	0
24	0	0	0	0	0	0	0	0	0	0	0	0	0	0	0	0	0	0	0	0	0	0	0	21	0	0	0	0	0	0
25	0	0	0	0	0	0	0	0	0	0	0	0	0	0	0	0	0	0	0	0	0	0	0	0	20	0	0	0	1	0
26	0	0	0	0	0	0	0	0	0	0	0	0	0	0	0	0	0	0	0	0	0	0	0	0	0	21	0	0	0	0
27	0	0	0	0	0	0	0	0	0	0	0	0	0	0	0	0	0	0	0	0	0	0	0	0	0	0	21	0	0	0
28	0	0	0	0	0	0	0	0	0	0	0	0	0	0	0	0	0	0	0	0	0	0	0	0	0	0	0	21	0	0
29	0	0	0	0	0	0	0	0	0	0	0	0	0	0	0	0	0	0	0	0	0	0	0	0	0	0	0	0	21	0
30	0	0	0	0	0	0	0	0	0	0	0	0	0	0	0	0	0	0	0	0	0	0	0	0	0	0	0	0	0	21

FIGURE 9. Confusion matrix obtained with the FrMT using adaptive nonlinear correlation. Rows represent true classes, while columns represent the predicted classes.

precision, the FrMT had slightly better performance than the FrST. With adaptive nonlinear correlation, both transformations performed similarly with all four metrics. The performance of both transforms with adaptive nonlinear correlation was better than that obtained with nonlinear correlation for mean accuracy, mean sensitivity, and mean precision. In contrast, mean specificity had the same performance in both types of correlations for both transformations.

Figures 6-9 present the confusion matrices for both transformations and both correlation types.

5. Conclusion

The results show similar performance across the two fractional transformations when using nonlinear correlation, achieving high performance across all metrics, with the FrMT performing slightly better than the FrST. In the case of adaptive nonlinear correlation, the results are the same for both transforms and are better than those obtained with nonlinear correlation. Therefore, the adaptive nonlinear correlation was the better option for both transformations. The results show that using fractional orders yields better discrimination performance for both transforms. Therefore, the fractional scale transform introduced in this work is a good new pattern recognition tool capable of scale-invariant identification with high performance.

The species analyzed determines the scale range used in this work. However, integral transformations of this type can be applied to a broader range, as demonstrated by Pech-Pacheco *et al*. (2003) [25], who used the classical scale transform to classify Arial font letters across scale ranges from 50% to 150%. Therefore, the fractional scale transform, being a generalization of the classical scale transform, can operate effectively over a broader range.

This methodology does not require a training stage; there is no need to know the scale, rotation, and position parameters in advance to achieve the performance reported in this work.

Conflicts of interest

The authors declare no conflict of interest related to this study.

Funding

This research was funded by Centro de Investigación Científica y de Educación Superior de Ensenada (CICESE), Baja California, grant number F0F181.

Data statement

The data supporting is not publicly available, but they can be shared if you send an Email to the corresponding author.

1. H. M. Ozaktas, M. A. Kutay, and D. Mendlovic, Introduction to the fractional Fourier transform and its applications, *In Advances in imaging and electron physics*, **106** (1999) 239, `https://doi.org/10.1016/S1076-5670(08)70272-6`
2. L. F. López-Ávila and J. Álvarez-Borrego, Fractional Fourier transform for digital image recognition, *International Journal of Pattern Recognition and Artificial Intelligence* **34** (2020),

https://doi.org/10.1142/S0218001420540257

3. E. Garza-Flores and J. Álvarez-Borrego, Pattern recognition using binary masks based on the fractional Fourier transform, *Journal of Modern Optics* **65** (2018) 1634, https://doi.org/10.1080/09500340.2018.1457186

4. O. Akay and G. F. Boudreaux-Bartels, Fractional Mellin transform: an extension of fractional frequency concept for scale, In Proc. 8th IEEE Digital Signal Processing Workshop, pages CD-ROM. IEEE (1998).

5. P. L. Butzer, A. A. Kilbas, and J. J. Trujillo, Fractional calculus in the Mellin setting and Hadamard-type fractional integrals, *Journal of Mathematical Analysis and Applications* **269** (2002) 1, https://doi.org/10.1016/S0022-247X(02)00001-X

6. P. L. Butzer, A. A. Kilbas, and J. J. Trujillo, Compositions of Hadamard-type fractional integration operators and the semigroup property, *Journal of Mathematical Analysis and Applications* **269** (2002) 387, https://doi.org/10.1016/S0022-247X(02)00049-5

7. P. L. Butzer, A. A. Kilbas, and J. J. Trujillo, Mellin transform analysis and integration by parts for Hadamard-type fractional integrals, *Journal of Mathematical Analysis and Applications* **270** (2002) 1, https://doi.org/10.1016/S0022-247X(02)00066-5

8. D. Casasent and D. Psaltis, Scale invariant optical transform, *Optical Engineering* **15** (1976) 258, https://doi.org/10.1117/12.7971962

9. D. Casasent and D. Psaltis, Position, rotation, and scale invariant optical correlation, *Applied Optics* **15** (1976) 1795, https://doi.org/10.1364/AO.15.001795

10. D. Sazbon *et al.*, Using Fourier/Mellin-based correlators and their fractional versions in navigational tasks, *Pattern Recognition* **35** (2002) 2993, https://doi.org/10.1016/S0031-3203(02)00018-3

11. V. D. Sharma, On the relationship between the fourier-mellin and the fractional fourier-mellin transform, *Bulletin of Pure & Applied Sciences-Mathematics and Statistics* **30** (2011) 251

12. X. Zuo and N. Zhou, Spectrum analysis on Mellin Transform and fractional Mellin transform, In 2011 4th International *Congress on Image and Signal Processing*, **4** (2011) 2218-2222, https://doi.org/10.1109/CISP.2011.6100534

13. N. Zhou *et al.*, Novel color image encryption algorithm based on the reality preserving fractional Mellin transform, *Optics & Laser Technology* **44** (2012) 2270, https://doi.org/10.1016/j.optlastec.2012.02.027

14. S. Vashisth *et al.*, Devil's vortex phase structure as frequency plane mask for image encryption using the fractional Mellin transform, *International Journal of Optics* **2014** (2014) 728056, https://doi.org/10.1155/2014/728056

15. V. D. Sharma and P. B. Deshmukh, Introduction to two dimensional fractional fourier-mellin transform, *International Journal of Research in Engineering and Applied Sciences* **5** (2015) 137

16. M. Baloch *et al.*, The Relationship of Fractional Laplace Transform with Fractional Fourier, Mellin and Sumudu Transforms, *American Scientific Research Journal for Engineering, Technology, and Sciences* **55** (2019) 11

17. M. Wang *et al.*, Image encryption scheme based on a Gaussian apertured reality-preserving fractional Mellin transform, *Optica Applicata* **50** (2020) 477, https://doi.org/10.37190/oa20012

18. L. Cohen, The scale representation, *IEEE Transactions on Signal Processing* **41** (1993) 3275, https://doi.org/10.1109/78.258073

19. A. Coronel-Beltrán and J. Álvarez-Borrego, Comparative analysis between different font types and letter styles using a nonlinear invariant digital correlation, *Journal of Modern Optics* **57** (2010) 58, https://doi.org/10.1080/09500340903511695

20. A. De Sena and D. Rocchesso, A fast Mellin and scale transform, *EURASIP Journal on Advances in Signal Processing* **2007** (2007) 089170, https://doi.org/10.1155/2007/89170

21. D. Casasent and D. Psaltis, New optical transforms for pattern recognition, *Proceedings of the IEEE* **65** (1977) 77, https://doi.org/10.1109/PROC.1977.10432

22. G. Cristobal, J. Cuesta, and L. Cohen, Image filtering and denoising through the scale transform, In Proceedings of the IEEE-SP International Symposium on Time-Frequency and Time-Scale Analysis (Cat. No. 98TH8380) (IEEE, 1998) pp. 617-620, https://doi.org/10.1109/TFSA.1998.721500

23. J. Álvarez-Borrego *et al.*, Invariant recognition of polychromatic images of Vibrio cholerae O1, *Optical Engineering* **41** (2002) 827, https://doi.org/10.1117/1.1456539

24. V. D. Sharma and P. B. Deshmukh, Applications of Two Dimensional Fractional Mellin Transform, *International Journal of Scientific and Innovative Mathematical Research* **2** (2014) 794

25. J. L. Pech-Pacheco *et al.*, Automatic object identification irrespective of geomatric changes, *Optical Engineering* **42** (2003) 551, https://doi.org/10.1117/1.1531189

26. S. Solorza and J. Álvarez-Borrego, Position and rotationinvariant pattern recognition system by binary rings masks, *Journal of Modern Optics* **62** (2015) 851, https://doi.org/10.1080/09500340.2015.1013579

27. A. S. Ventura, J. Álvarez-Borrego, and S. Solorza, Adaptive nonlinear correlation with a binary mask invariant to rotation and scale, *Optics Communications* **339** (2015) 185, https://doi.org/10.1016/j.optcom.2014.11.051